**Chemistry of Metals and Alloys**

*Chem. Met. Alloys* 1 (2008) 76-83
Ivan Franko National University of Lviv
www.chemetal-journal.org

# $Ce_6ZnBi_{14}$ and $Pr_6InSb_{15}$: Ternary rare-earth intermetallics with extended pnicogen ribbons

Andriy V. TKACHUK[1], Thomas TAM[1], Arthur MAR[1]*

[1] *Department of Chemistry, University of Alberta, Edmonton, Alberta, Canada T6G 2G2,*
** Corresponding author. Fax: +1 780 492 8231; e-mail: arthur.mar@ualberta.ca*

Received January 31, 2008; accepted February 17, 2008; available on-line March 31, 2008

**The ternary rare-earth pnictides $Ce_6ZnBi_{14}$ and $Pr_6InSb_{15}$ have been prepared by reaction of the elements at 950 °C. Their crystal structures were determined by single-crystal X-ray diffraction ($Ce_6ZnBi_{14}$, Pearson symbol *oI*42, orthorhombic, space group *Immm*, $Z = 2$, $a = 4.3916(4)$ Å, $b = 15.399(1)$ Å, $c = 19.315(2)$ Å; $Pr_6InSb_{15}$, Pearson symbol *oI*44, orthorhombic, space group *Immm*, $Z = 2$, $a = 4.2373(3)$ Å, $b = 15.037(1)$, $c = 19.337(1)$ Å). $Ce_6ZnBi_{14}$ and $Pr_6InSb_{15}$ can be considered to be stuffed variants of the $(U_{0.5}Ho_{0.5})_3Sb_7$ and $La_6MnSb_{15}$ structure types, respectively, in which square pyramidal sites are partially occupied by Zn or In atoms. All of these compounds are characterized by extensive homoatomic bonding of the pnicogen (Sb or Bi) atoms within the anionic substructure.**

**Pnictide / Intermetallics / Crystal structure**

## Introduction

The structures of many rare-earth Sb-rich intermetallic compounds contain several types of anionic networks of Sb atoms in the form of ribbons and square nets [1]. Electron-counting rules have now been well established to account for the hypervalent Sb–Sb bonding within these Sb substructures, and can be extended to compounds of other main-group elements, primarily the heavier pnictides and chalcogenides [2, 3]. A difficulty in applying these rules is that there is often a wide range of intermediate Sb–Sb interactions (2.9–3.5 Å) so that it is not clear that they can be associated with integer electron counts. Moreover, these Sb networks are frequently subject to distortions, rendering structural determinations to be challenging. Examples of these anionic Sb networks are now plentiful, but much rarer are the corresponding polybismuthides, because it is less likely for Bi to adopt a formally negative oxidation state [4].

The $La_6MnSb_{15}$-type structure, adopted by $RE_6MSb_{15}$ (*RE* = La, Ce; *M* = Mn, Cu, Zn) [5], exemplifies this complexity, with its variety of Sb substructures whose bonding can be understood through a "retrotheoretical" or fragment analysis [6]. In $La_6MnSb_{15}$, the Mn atoms can be considered to occupy interstitial sites of distorted tetrahedral geometry within the anionic framework. A closely related structure type is $(U_{0.5}Ho_{0.5})_3Sb_7$, adopted by the pseudo-binaries $(U_{0.5}RE_{0.5})_3Sb_7$ (*RE* = Y, Gd–Ho), where similar interstitial sites remain empty [7]. Recognizing relationships between defect and stuffed structures is a common strategy for targeting new solid-state compounds. We recently prepared $La_{12}Ga_{3.5}Mn_{0.5}Sb_{23.5}$ [8], which may be considered to be a stuffed variant of the $RE_{12}Ga_4Sb_{23}$-type structure [9]. Here, we report two new ternary rare-earth pnictides, $Ce_6ZnBi_{14}$ and $Pr_6InSb_{15}$, whose structures may be regarded as stuffed variants of $(U_{0.5}Ho_{0.5})_3Sb_7$ and $La_6MnSb_{15}$, respectively, but with a different site, of square pyramidal geometry, being occupied.

## Experimental

*Synthesis*

Starting materials were Ce (99.9 %, Alfa-Aesar), Pr (99.9 %, Cerac), Zn (99.999 %, Cerac), In (99.99 %, Aldrich), Bi (99.999 %, Alfa-Aesar), and Sb (99.999 %, Alfa-Aesar). Mixtures of the elements were placed within evacuated fused-silica tubes and heated in a furnace. $Ce_6ZnBi_{14}$ was prepared from a stoichiometric mixture of the elements. The tube was heated at 500 °C for 48 h and 950 °C for 48 h, cooled to 600 °C over 96 h, and then cooled to room temperature over 24 h. Small thin needles of $Ce_6ZnBi_{14}$ were obtained. $Pr_6InSb_{15}$ was identified as a byproduct from a reaction intended for the preparation of "$PrIn_{0.8}Sb_2$" [10]. The tube was heated at 570 °C for 24 h and 950 °C for 48 h, cooled to 500 °C over 24 h, and then cooled to room temperature over 5 h. Crystals of $Pr_6InSb_{15}$, which are

needle-shaped, are readily distinguished from $PrIn_{0.8}Sb_2$, which are plate-shaped. Efforts to optimize the synthesis of $Pr_6InSb_{15}$ and to prepare other rare-earth analogues of both $Ce_6ZnBi_{14}$ and $Pr_6InSb_{15}$ are ongoing. Energy-dispersive X-ray (EDX) analyses on a Hitachi S-2700 scanning electron microscope confirmed that the elemental compositions are in good agreement with those from the X-ray structure determination.

*Structure determination*

Intensity data for $Ce_6ZnBi_{14}$ and $Pr_6InSb_{15}$ were collected on a Bruker Platform / SMART 1000 CCD diffractometer at 22 °C using ω scans. Crystal data and further details of the data collection are given in Table 1. Calculations were carried out with use of the SHELXTL (version 6.12) package [11]. Face-indexed numerical absorption corrections were applied. For both compounds, the centrosymmetric space group *Immm* was chosen and initial atomic positions of the rare-earth and pnicogen atoms were readily found by direct methods. The resemblance to the structures of $(U_{0.5}Ho_{0.5})_3Sb_7$ [7] and $La_6MnSb_{15}$ [5] became immediately apparent. For ease of comparison, the atomic positions were standardized relative to $(U_{0.5}Ho_{0.5})_3Sb_7$, which can be considered to be the basic host structure [7]. The remaining atoms were identified from difference electron density maps.

In $Ce_6ZnBi_{14}$, the Zn atoms were located in a square pyramidal site (4*j*). The position of Bi5 is shifted to a site of lower symmetry (4*f*: 0.39, 1/2, 0) compared to that of Sb5 (2*c*: 1/2, 1/2, 0) in $(U_{0.5}Ho_{0.5})_3Sb_7$, which results in distances that are too short to another symmetry-equivalent Bi5 site at 0.9 Å and to a Zn site at 2.2 Å. When the occupancies of these sites were refined freely, they converged to 0.53(2) for Zn and 0.48(1) for Bi5, and the displacement parameters became more reasonable. Refinement of the occupancies for the other sites confirmed that they are essentially fully occupied, with values ranging from 0.98(5) to 1.02(5). In the final refinement of $Ce_6ZnBi_{14}$, the occupancies were fixed at 0.50 for Zn and Bi5, and at 1.00 for all other sites.

**Table 1** Crystallographic data for $Ce_6ZnBi_{14}$ and $Pr_6In_{0.89(1)}Sb_{15}$.

| | | |
|---|---|---|
| Formula | $Ce_6ZnBi_{14}$ | $Pr_6In_{0.89(1)}Sb_{15}$ |
| Formula mass (amu) | 3831.81 | 2773.90 |
| Space group | *Immm* (No. 71) | *Immm* (No. 71) |
| *a* (Å) | 4.3916(4) | 4.2373(3) |
| *b* (Å) | 15.399(1) | 15.037(1) |
| *c* (Å) | 19.315(2) | 19.337(1) |
| *V* (Å$^3$) | 1306.2(2) | 1232.1(1) |
| *Z* | 2 | 2 |
| $\rho_{calcd}$ (g cm$^{-3}$) | 9.743 | 7.477 |
| Crystal dimensions (mm) | $0.11 \times 0.03 \times 0.02$ | $0.14 \times 0.03 \times 0.02$ |
| Radiation | Graphite monochromated Mo *K*α, λ = 0.71073 Å | |
| μ(Mo *K*α) (cm$^{-1}$) | 1049.86 | 285.22 |
| Transmission factors | 0.026–0.162 | 0.046–0.558 |
| 2θ limits | $3.38° \le 2\theta(\text{Mo } K\alpha) \le 66.18°$ | $3.44° \le 2\theta(\text{Mo } K\alpha) \le 66.26°$ |
| Data collected | $-6 \le h \le 6$, $-23 \le k \le 23$, $-29 \le l \le 29$ | $-6 \le h \le 6$, $-22 \le k \le 22$, $-29 \le l \le 29$ |
| No. of data collected | 8625 | 8153 |
| No. of unique data, including $F_o^2 < 0$ | 1428 | 1363 |
| No. of unique data, with $F_o^2 > 2\sigma(F_o^2)$ | 1053 | 1182 |
| No. of variables | 43 | 47 |
| $R(F)$ for $F_o^2 > 2\sigma(F_o^2)$ [a] | 0.041 | 0.034 |
| $R_w(F_o^2)$ [b] | 0.085 | 0.077 |
| Goodness of fit | 1.064 | 1.102 |
| $(\Delta\rho)_{max}$, $(\Delta\rho)_{min}$ (e Å$^{-3}$) | 7.18, –4.09 | 4.84, –5.24 |

[a] $R(F) = \sum \big||F_o| - |F_c|\big| \Big/ \sum |F_o|$.

[b] $R_w(F_o^2) = \left[\sum \left[ w(F_o^2 - F_c^2)^2 \right] \Big/ \sum w F_o^4 \right]^{1/2}$; $w^{-1} = \left[\sigma^2(F_o^2) + (Ap)^2 + Bp\right]$ where $p = \left[\max(F_o^2, 0) + 2F_c^2\right]/3$.

In $Pr_6InSb_{15}$, the In atoms were located in square pyramidal In1 (4*j*) and tetrahedral In2 (4*h*) sites. The position of Sb5 is split into two closely-spaced but distinct sites, Sb5a (2*c*: 1/2, 1/2, 0) and Sb5b (4*f*: 0.40, 1/2, 0). The In1, Sb5a, and Sb5b sites cannot be simultaneously fully occupied because of short distances to symmetry-equivalent positions. Refinement of the occupancies of these sites, with the constraint that the sum of these occupancies cannot exceed 1.00, resulted in values of 0.57(1) for Sb5a, 0.30(1) for Sb5b, and 0.13(1) for In1. All other sites are fully occupied (0.98(1)–0.99(1)), except for In2, which is partially occupied at 0.32(1). To arrive at a simple model for a local interpretation of this disorder, the occupancies were fixed at 0.50 for Sb5a, 0.25 for Sb5b, 0.125 for In1, and 1.00 for all other atoms except for In2, whose occupancy was refined freely. The final formula is $Pr_6In_{0.89(1)}Sb_{15}$, but for simplicity, we will refer to it as $Pr_6InSb_{15}$.

For both structures, the possibility of lower symmetry space groups (*Imm*2 and its permutations, *I*222, and $I2_12_12_1$) was investigated, but refinements did not support an ordered model in which the three-atom-wide *Pn* ribbons (containing the problematic *Pn*5 sites) are distorted exclusively in one direction, as occurs in $La_6MnSb_{15}$ (*Imm*2) [5]. Final values of the positional and displacement parameters are given in Table 2. Interatomic distances are listed in Table 3. Further data, in the form of a Crystallographic Information File (CIF), have been sent to Fachinformationszentrum Karlsruhe, Abt. PROKA, 76344 Eggenstein-Leopoldshafen, Germany, as supplementary material No. CSD-419305 and 419306 and can be obtained by contacting FIZ (quoting the article details and the corresponding CSD numbers).

*Electrical resistivity*

The electrical resistivity of needle-shaped single crystals of $Pr_6InSb_{15}$ was measured by standard four-probe techniques on a Quantum Design PPMS system equipped with an ac transport controller (Model 7100). The crystals were about 0.4 mm in length and attached with silver paint on gold wires with graphite extensions. The current was 100 μA and the frequency was 16 Hz.

**Table 2** Positional and equivalent isotropic displacement parameters for $Ce_6ZnBi_{14}$ and $Pr_6In_{0.89(1)}Sb_{15}$.

| Atom | Wyckoff position | occupancy | *x* | *y* | *z* | $U_{eq}$ (Å$^2$) [a] |
|---|---|---|---|---|---|---|
| $Ce_6ZnBi_{14}$ | | | | | | |
| Ce1 | 8*l* | 1 | 0 | 0.14195(6) | 0.36665(5) | 0.0097(2) |
| Ce2 | 4*i* | 1 | 0 | 0 | 0.17114(7) | 0.0109(3) |
| Zn | 4*j* | 0.500 | 1/2 | 0 | 0.4323(3) | 0.016(1) |
| Bi1 | 8*l* | 1 | 0 | 0.21146(4) | 0.19673(4) | 0.0109(2) |
| Bi2 | 8*l* | 1 | 0 | 0.36165(4) | 0.41028(4) | 0.0158(2) |
| Bi3 | 4*j* | 1 | 1/2 | 0 | 0.29837(5) | 0.0125(2) |
| Bi4 | 4*g* | 1 | 0 | 0.32737(6) | 0 | 0.0142(2) |
| Bi5 | 4*f* | 0.500 | 0.3942(4) | 1/2 | 0 | 0.0128(4) |
| Bi6 | 2*a* | 1 | 0 | 0 | 0 | 0.0190(3) |
| $Pr_6In_{0.89(1)}Sb_{15}$ | | | | | | |
| Pr1 | 8*l* | 1 | 0 | 0.13999(3) | 0.36676(2) | 0.0067(1) |
| Pr2 | 4*i* | 1 | 0 | 0 | 0.17726(3) | 0.0086(1) |
| In1 | 4*j* | 0.125 | 1/2 | 0 | 0.4372(5) | 0.023(2) |
| In2 | 4*h* | 0.319(5) | 0 | 0.2757(2) | 1/2 | 0.019(1) |
| Sb1 | 8*l* | 1 | 0 | 0.21479(4) | 0.20253(3) | 0.0077(1) |
| Sb2 | 8*l* | 1 | 0 | 0.35853(4) | 0.39359(3) | 0.0134(1) |
| Sb3 | 4*j* | 1 | 1/2 | 0 | 0.30227(4) | 0.0076(2) |
| Sb4 | 4*g* | 1 | 0 | 0.33824(7) | 0 | 0.0153(2) |
| Sb5a | 2*c* | 0.500 | 1/2 | 1/2 | 0 | 0.0084(3) [b] |
| Sb5b | 4*f* | 0.250 | 0.4029(8) | 1/2 | 0 | 0.0084(3) [b] |
| Sb6 | 4*g* | 1 | 0 | 0.09758(7) | 0 | 0.0179(2) |

[a] $U_{eq}$ is defined as one-third of the trace of the orthogonalized $U_{ij}$ tensor.
[b] Constrained with isotropic displacement parameters of equal magnitude.

**Table 3** Selected interatomic distances (Å) in $Ce_6ZnBi_{14}$ and $Pr_6InSb_{15}$.

| | | | |
|---|---|---|---|
| $Ce_6ZnBi_{14}$ | | | |
| Ce1–Bi3 | 3.367(1) (×2) | Bi1–Bi2 | 3.219(1) (×2) |
| Ce1–Bi1 | 3.379(1) (×2) | Bi1–Bi1 | 3.235(1) (×2) |
| Ce1–Bi5 | 3.410(1) (×2) | Bi2–Bi1 | 3.219(1) (×2) |
| Ce1–Bi4 | 3.417(1) (×2) | Bi2–Bi2 | 3.466(2) |
| Ce1–Bi1 | 3.452(1) | Bi2–Bi6 | 3.516(1) (×2) |
| Ce1–Bi2 | 3.487(1) | Bi4–Bi5 | 3.172(1) (×2) |
| Ce1–Zn | 3.348(2) (×2) | Bi4–Bi5 | 3.761(1) (×2) |
| Ce2–Bi1 | 3.294(1) (×2) | Bi5–Bi4 | 3.172(1) (×2) |
| Ce2–Bi3 | 3.295(1) (×2) | Bi5–Bi5 | 3.462(4) |
| Ce2–Bi6 | 3.306(1) | Bi5–Bi4 | 3.761(1) (×2) |
| Ce2–Bi2 | 3.440(1) (×4) | Bi6–Bi2 | 3.516(1) (×8) |
| Zn–Bi3 | 2.587(6) | | |
| Zn–Bi4 | 2.963(3) (×2) | | |
| Zn–Bi5 | 2.965(3) (×2) | | |
| Zn–Zn | 2.615(12) | | |
| $Pr_6InSb_{15}$ | | | |
| Pr1–Sb3 | 3.236(1) (×2) | Sb1–Sb1 | 2.997(1) (×2) |
| Pr1–Sb1 | 3.324(1) (×2) | Sb1–Sb2 | 3.026(1) (×2) |
| Pr1–Sb2 | 3.327(1) | Sb2–Sb6 | 3.026(1) (×2) |
| Pr1–Sb5a | 3.327(1) | Sb2–Sb1 | 3.026(1) (×2) |
| Pr1–Sb4 | 3.352(1) (×2) | Sb4–Sb5b | 2.972(2) (×2) |
| Pr1–Sb5b | 3.352(1) (×2) | Sb4–Sb5a | 3.226(1) (×2) |
| Pr1–In1 | 3.283(4) (×2) | Sb4–Sb5b | 3.510(2) (×2) |
| Pr1–In2 | 3.286(2) | Sb4–Sb6 | 3.619(1) |
| Pr2–Sb3 | 3.214(1) (×2) | Sb5a–Sb4 | 3.226(1) (×4) |
| Pr2–Sb1 | 3.267(1) (×2) | Sb5a–Sb5b | 3.826(2) (×2) |
| Pr2–Sb2 | 3.300(1) (×4) | Sb5b–Sb4 | 2.972(2) (×2) |
| Pr2–Sb6 | 3.729(1) (×2) | Sb5b–Sb4 | 3.510(2) (×2) |
| In1–Sb5b | 2.806(5) (×2) | Sb5b–Sb5b | 3.414(2) |
| In1–Sb4 | 2.718(4) (×2) | Sb6–Sb6 | 2.935(2) |
| In1–Sb3 | 2.609(10) | Sb6–Sb2 | 3.026(1) (×4) |
| In2–Sb2 | 2.405(2) (×2) | Sb6–Sb4 | 3.619(1) |
| In2–Sb4 | 2.725(2) (×2) | | |
| In2–Sb6 | 2.850(2) (×2) | | |

## Results and discussion

$Ce_6ZnBi_{14}$ and $Pr_6InSb_{15}$ adopt new structures types, shown in Fig. 1, containing a rich variety of polyanionic networks. The pnicogen atoms are arranged in four-atom-wide (*Pn*2–*Pn*1–*Pn*1–*Pn*2) and three-atom-wide (*Pn*4–*Pn*5–*Pn*4) ribbons extending down the *a* direction. The four-atom-wide ribbons are connected by single Bi6 atoms in $Ce_6ZnBi_{14}$ or by Sb6–Sb6 pairs in $Pr_6InSb_{15}$ to form an extended network outlining large channels. These channels contain face-sharing columns of trigonal prisms with *RE* atoms at the vertices and single *Pn*3 atoms at the centres. There remain square pyramidal sites that are partially occupied by Zn atoms in $Ce_6ZnBi_{14}$ or In1 atoms in $Pr_6InSb_{15}$. In addition, there are distorted tetrahedral sites in $Pr_6InSb_{15}$ that are partially occupied by In2 atoms. The only other compounds previously identified in the *RE*–Zn–Bi and *RE*–In–Sb systems are $Yb_9Zn_4Bi_9$ [12] and $REIn_{0.8}Sb_2$ (*RE* = La–Nd) [10], respectively, but there is little resemblance to the structures shown here except for the occurrence in $LaIn_{0.8}Sb_2$ of square Sb nets from which pnicogen ribbons can be considered to be excised.

In $Ce_6ZnBi_{14}$, the Zn and Bi5 sites are each only half-occupied, which entails a disorder within the three-atom-wide Bi ribbons. Fig. 2 illustrates one possible local interpretation for the disorder within

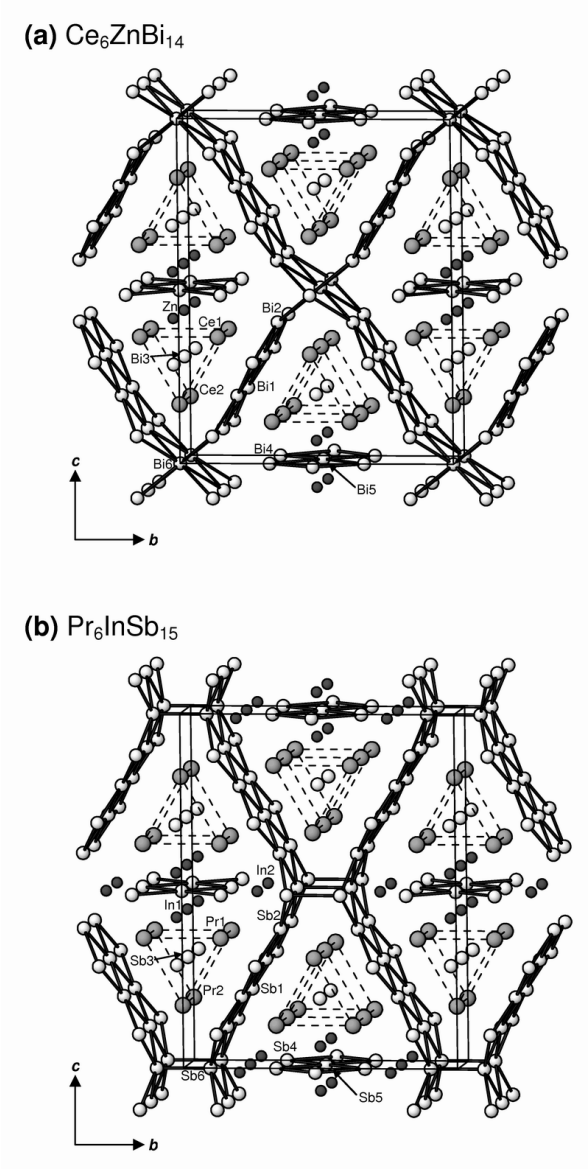


**Fig. 1** Structure of (a) $Ce_6ZnBi_{14}$ and (b) $Pr_6InSb_{15}$ viewed down the *a* direction. The large grey spheres are *RE* atoms, the small solid spheres are Zn or In atoms, and the medium lightly-shaded spheres are Bi or Sb atoms. The dashed lines outline the $RE_6$ trigonal prisms.

these ribbons, in which the $Bi_4$ squares extending along the *a* direction are alternately small (Bi–Bi, 3.172(1) Å) or large (Bi–Bi, 3.761(1) Å). (Because the Bi–Bi–Bi angles are not strictly 90º, these are really $Bi_4$ rhombi, but are referred to as squares for simplicity.) Reasonable Zn–Bi distances (2.587(6)–2.965(3) Å) can be attained only if the larger $Bi_4$ squares within these ribbons are capped by Zn atoms. Capping on both sides of a large $Bi_4$ square is permissible because the resulting Zn–Zn distance of 2.62(1) Å is still consistent with that found in the elemental Zn (2.644 Å) [13]. The shifting of the

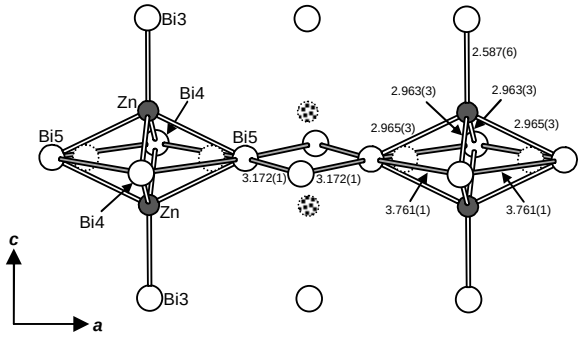


**Fig. 2** One possible local ordering of the half-occupied Zn and Bi5 sites within the three-atom-wide Bi ribbons in $Ce_6ZnBi_{14}$.

central Bi atom within the three-atom-wide Bi ribbons is reminiscent of a similar phenomenon in the three-atom-wide Sb ribbons in $La_6MnSb_{15}$ [5], where each of the $Sb_4$ squares is squashed on one side because of a Peierls-type sliding distortion [6].

In $Pr_6InSb_{15}$, the disorder within the three-atom-wide Sb ribbons is rather more complex. There are now two sets of sites for the central Sb atom, at Sb5a (2*c*; occupancy 0.50) and Sb5b (4*f*; occupancy 0.25), while the In1 site has an occupancy of 0.125. Fig. 3 illustrates the three possible scenarios for a local interpretation for this disorder. If the Sb5a sites are occupied, all of the $Sb_4$ squares within the ribbon are identical (Sb–Sb, 3.226(1) Å) and none of the In1 sites are occupied. If the Sb5b sites are occupied, the situation devolves to one similar to the Bi ribbons in $Ce_6ZnBi_{14}$, with alternately small (Sb–Sb, 2.972(2) Å) or large (Sb–Sb, 3.510(2) Å) $Sb_4$ squares extending along the *a* direction. Only the larger $Sb_4$ squares are capped by In1 atoms, giving In–Sb distances of 2.609(10)–2.806(5) Å. However, capping on both sides of the large $Sb_4$ square by In1 atoms is now precluded because the resulting In1–In1 distances of 2.43(2) Å would be too short. Of course, the orientation of the $InSb_5$ square pyramids need not be "all up" as in Fig. 3b or "all down" as in Fig. 3c, but could well be random on proceeding along the length of the Sb ribbon.

A second indium site, In2, is partially occupied at 0.32(1). The unusual coordination geometry of this site, a distorted tetrahedron with two additional capping Sb atoms, has been identified previously in $RE_6MSb_{15}$ compounds [5, 6]. It appears that the interstitial atoms that enter this site are typically those that have formally $d^5$ ($Mn^{2+}$) or $d^{10}$ configuration ($Cu^+$, $Zn^{2+}$), probably because they introduce only a minimal perturbation to the bonding energy of anionic substructure [6]. The implication from this argument is that the indium atoms here also have a $d^{10}$ configuration and can be formally counted as $In^{3+}$. It is interesting to note that in the well-known family of $A_{14}MPn_{11}$ phases with the $Ca_{14}AlSb_{11}$ structure type [14], the *M* atoms that can be substituted are also Mn, Zn, Cd, Al, Ga, and In [15].

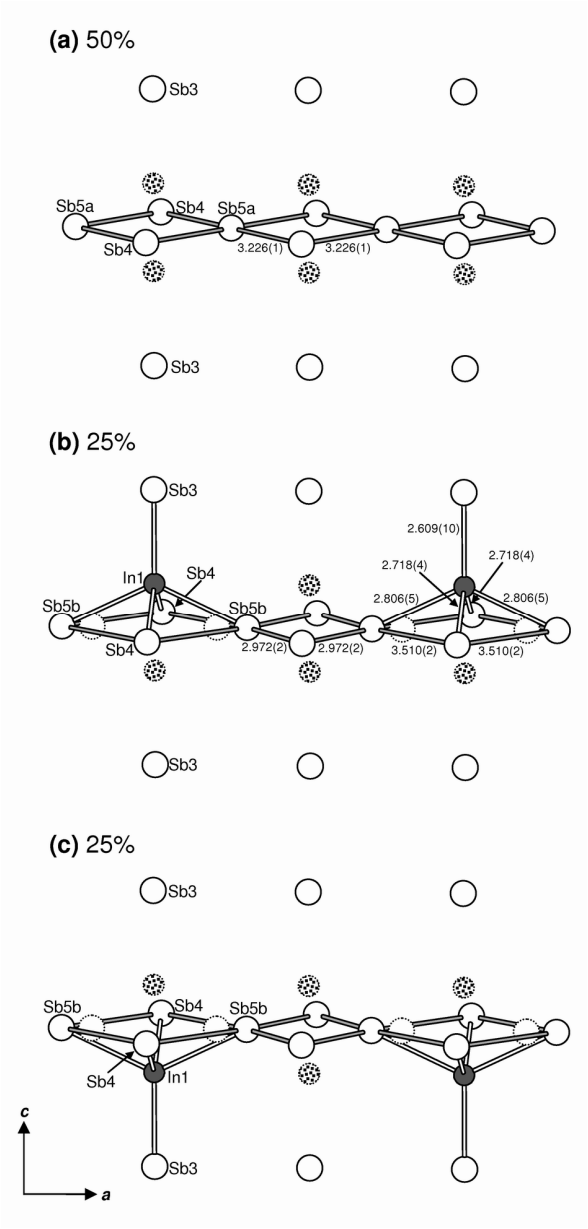


**Fig. 3** Three possible local orderings of the partially occupied In1, Sb5a, and Sb5b sites within the three-atom-wide Sb ribbons in $Pr_6InSb_{15}$. The percentages indicate the probability of each scenario.

Despite their seemingly complex compositions, the structures of $Ce_6ZnBi_{14}$ and $Pr_6InSb_{15}$ can be readily related to those of $(U_{0.5}Ho_{0.5})_3Sb_7$ [7] and $La_6MnSb_{15}$ [5], as shown in Fig. 4, by deconstructing the pnicogen networks and by enumerating the occupation of interstitial sites, as summarized in Table 4. All four structures contain rare-earth trigonal prisms centred by isolated pnicogen atoms, and two types of *Pn* ribbons. The four-atom-wide *Pn* ribbons are connected by single *Pn* atoms in $(U_{0.5}Ho_{0.5})_3Sb_7$ and $Ce_6ZnBi_{14}$, or by *Pn*–*Pn* pairs in $La_6MnSb_{15}$ and $Pr_6InSb_{15}$. If $(U_{0.5}Ho_{0.5})_3Sb_7$ is considered to be the host structure, then partial filling of the square pyramidal sites leads to $Ce_6ZnBi_{14}$, partial filling of the tetrahedral sites leads to $La_6MnSb_{15}$, and partially filling of both types of sites leads to $Pr_6InSb_{15}$.

A detailed description of the bonding in $Ce_6ZnBi_{14}$ and $Pr_6InSb_{15}$ is not easy to formulate. The rare-earth atoms are almost certainly trivalent (i.e., $Ce^{3+}$, $Pr^{3+}$), and as alluded to earlier, the interstitial atoms probably have filled d subshells (i.e., $Zn^{2+}$, $In^{3+}$). For a four-bonded *Pn* atom within a square net, simple electron counting rules suggest a formal charge of $Pn^{1-}$, where an octet is achieved by assigning two lone pairs on each atom and assuming the *Pn*–*Pn* contacts to be one-electron bonds [2]. However, the presence of numerous intermediate *Pn*–*Pn* interactions makes such an assignment problematic. As first suggested by Jeitschko et al. [16], a bond valence calculation can be applied to obtain non-integral formal charges on the *Pn* atoms, using the equation $\nu_{ij} = \exp[(R_{ij} - d_{ij})/0.37]$ for the bond order of a *Pn*–*Pn* interaction, where $R_{ij}$ is the bond-valence parameter and $d_{ij}$ is the distance in Å [17]. When $R_{ij}$ is chosen to be 2.80 Å for Sb–Sb interactions, which was optimized for binary rare-earth polyantimonides [16], the formal charges in $Pr_6InSb_{15}$ are found to be –0.7 on Sb1, –0.7 on Sb2, –3.0 on Sb3, –2.1 to –2.7 on Sb4, –1.7 on Sb5a, –1.5 on Sb5b, and –0.1 on Sb6, consistent with the expectation that Sb atoms participating in a greater number of homoatomic bonds acquire a less negative charge. The total formal charge for all the Sb atoms is –19 per formula unit, which is in fair agreement with the compensating positive charge of +21 assuming six $Pr^{3+}$ and one $In^{3+}$ per formula unit. It must be recognized that the values of $\nu_{ij}$ are sensitive to the choice on the parameter $R_{ij}$. A similar analysis can be made for the Bi atoms in $Ce_6ZnBi_{14}$. No guidelines are available from other polybismuthides, but if the $R_{ij}$ value of 3.08 Å listed from O'Keeffe and Brese [18] for Bi–Bi interactions is assumed to be overestimated by the same amount (0.2 Å) as for Sb–Sb contacts, then a value of 3.06 Å can be tried. This leads to formal charges of –0.5 for Bi1, –1.2 for Bi2, –3.0 for Bi3, –2.1 for Bi4, –1.2 for Bi5, and –0.7 for Bi6. The total formal charge for all the Bi atoms is also –19 per formula unit, in good agreement with the compensating positive charge of +20 from the six $Ce^{3+}$ and one $Zn^{2+}$ per formula unit.

Both $Ce_6ZnBi_{14}$ and $Pr_6InSb_{15}$ are expected to display metallic behaviour. The electrical resistivity of $Pr_6InSb_{15}$ is plotted in Fig. 5. It shows only weak temperature dependence, consistent with the large scattering of conduction electrons that arises from the considerable disorder in the structure. There is an abrupt decrease in resistivity below 3.8 K. Although the resistivity measurements were performed on single crystals confirmed to be $Pr_6InSb_{15}$ by EDX analysis, it should be noted that elemental indium undergoes a superconducting transition at 3.4 K, so its presence must be definitively ruled out before any conclusions can be drawn.

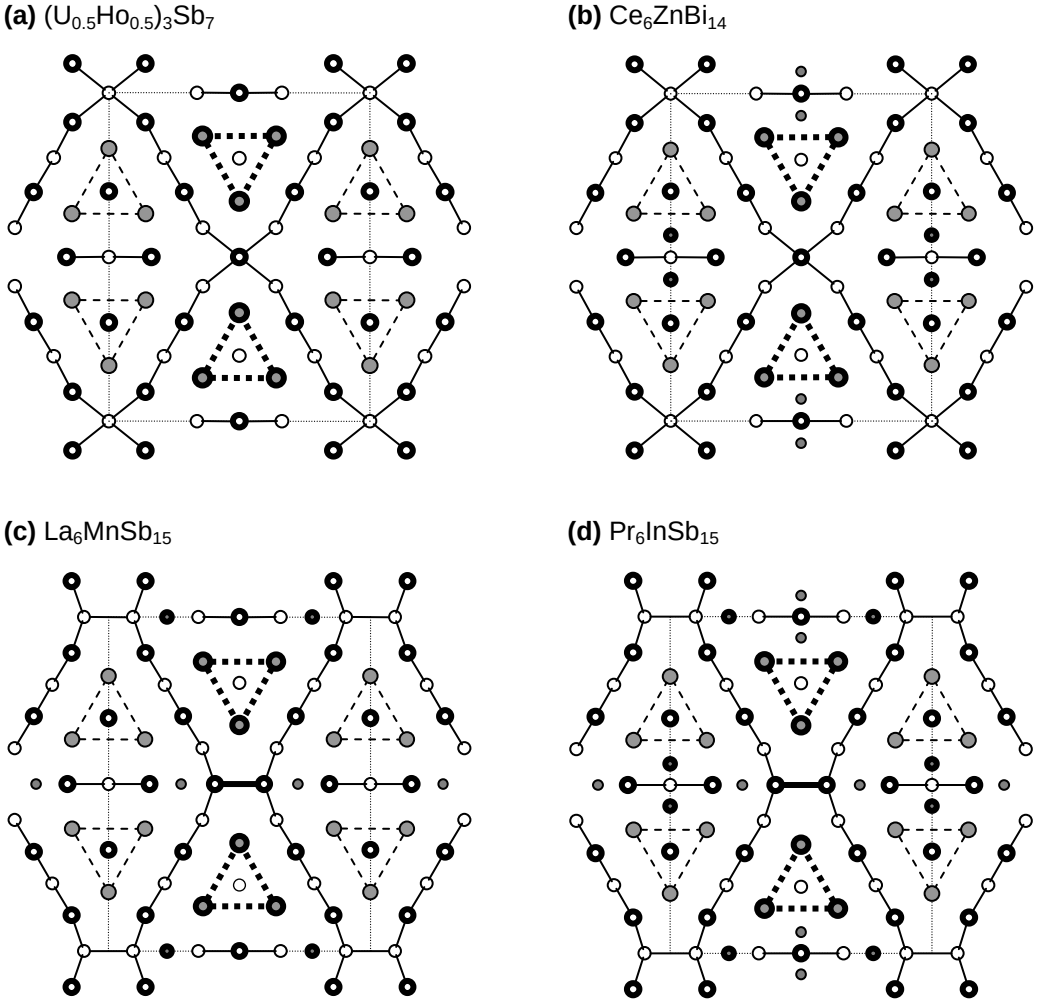


**Fig. 4** Comparison of the orthorhombic structures of (a) $(U_{0.5}Ho_{0.5})_3Sb_7$, (b) $Ce_6ZnBi_{14}$, (c) $La_6MnSb_{15}$, and (d) $Pr_6InSb_{15}$, shown in projection down the shortest axis. The large lightly-shaded circles are *RE* atoms, the small solid circles are Zn, Mn, or In atoms, and the medium open circles are Sb or Bi atoms. Circles with thicker rims indicate atoms residing in planes displaced by 1/2 the short axis parameter.

**Table 4** Relationship among ternary rare-earth pnictides

| Compound | $4 \times (U_{0.5}Ho_{0.5})_3Sb_7 = (U_{0.5}Ho_{0.5})_{12}Sb_{28}$ | $2 \times Ce_6ZnBi_{14} = Ce_{12}Zn_2Bi_{28}$ | $2 \times La_6MnSb_{15} = La_{12}Mn_2Sb_{30}$ | $2 \times Pr_6In_{0.89}Sb_{15} = Pr_{12}In_{1.8}Sb_{30}$ |
|---|---|---|---|---|
| Trigonal prisms | 6 U + 6 Ho | 12 Ce | 12 La | 12 Pr |
| Square pyramidal sites (4*j*) | --- | $0.5 \times 4$ Zn = 2 Zn | --- | $0.125 \times 4$ In = 0.5 In |
| Tetrahedral sites (4*h*) | --- | --- | $0.5 \times 4$ Mn = 2 Mn | $0.319 \times 4$ In = 1.3 In |
| Four-atom-wide *Pn* ribbons | 16 Sb | 16 Bi | 16 Sb | 16 Sb |
| Three-atom-wide *Pn* ribbons | 6 Sb | 6 Bi | 6 Sb | 6 Sb |
| *Pn*–*Pn* pairs | --- | --- | 4 Sb | 4 Sb |
| Single *Pn* atoms in pnicogen network | 2 Sb | 2 Bi | --- | --- |
| Single *Pn* atoms in trigonal prisms | 4 Sb | 4 Bi | 4 Sb | 4 Sb |

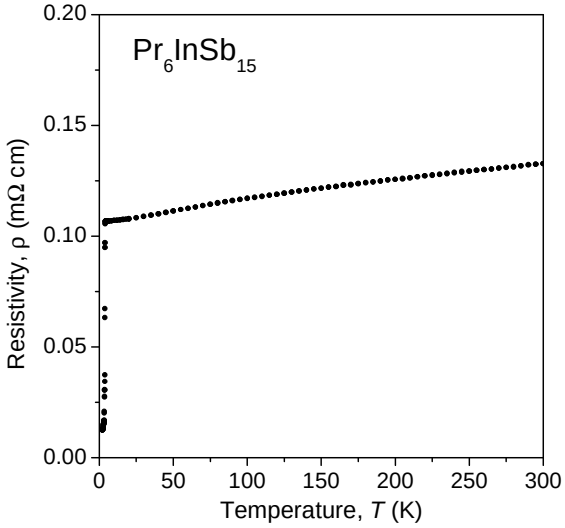


**Fig. 5** Electrical resistivity measured along the needle axis (parallel to *a*) of $Pr_6InSb_{15}$.

The two compounds described here demonstrate the continuing appeal of pnicogen ribbons as a simple principle to organize the structures of polyantimonides, and now polybismuthides. It will be interesting to see if other atoms with $d^{10}$ configuration can be inserted into the interstitial sites within the anionic framework. It will also be worthwhile to investigate the magnetic properties as different rare-earth elements are substituted.

**Acknowledgment**

The Natural Sciences and Engineering Research Council of Canada and the University of Alberta supported this work. We thank Dr. Robert McDonald and Dr. Michael J. Ferguson (Faculty Service Officer, X-ray Crystallography Laboratory) for the X-ray data collection.

**References**

[1] A.M. Mills, R. Lam, M.J. Ferguson, L. Deakin, A. Mar, *Coord. Chem. Rev.* 233–234 (2002) 207-222.
[2] G.A. Papoian, R. Hoffmann, *Angew. Chem. Int.* Ed. 39 (2000) 2408-2448.
[3] G. Papoian, R. Hoffmann, *J. Am. Chem. Soc.* 123 (2001) 6600-6608.
[4] M.G. Morgan, M. Wang, W.Y. Chan, A. Mar, *Inorg. Chem.* 42 (2003) 1549-1555.
[5] O. Sologub, M. Vybornov, P. Rogl, K. Hiebl, G. Cordier, P. Woll, *J. Solid State Chem.* 122 (1996) 266-272.
[6] G. Papoian, R. Hoffmann, *J. Solid State Chem.* 139 (1998) 8-21.
[7] T. Schmidt, W. Jeitschko, *Inorg. Chem.* 40 (2001) 6356-6361.
[8] S.J. Crerar, M.G. Morgan, A. Mar, *J. Solid State Chem.* 171 (2003) 137-142.
[9] A.M. Mills, A. Mar, *Inorg. Chem.* 39 (2000) 4599-4607.
[10] M.J. Ferguson, R.E. Ellenwood, A. Mar, *Inorg. Chem.* 38 (1999) 4503-4509.
[11] G.M. Sheldrick, *SHELXTL, Version 6.12*, Bruker AXS Inc., Madison, WI, 2001.
[12] S.-J. Kim, J. Salvador, D. Bilc, S.D. Mahanti, M.G. Kanatzidis, *J. Am. Chem. Soc.* 123 (2001) 12704-12705.
[13] J. Donohue, *The Structures of the Elements*, Wiley, New York, 1974.
[14] G. Cordier, H. Schäfer, M. Stelter, *Z. Anorg. Allg. Chem.* 519 (1984) 183-188.
[15] S.M. Kauzlarich, in: S.M. Kauzlarich (Ed.), *Chemistry, Structure, and Bonding of Zintl Phases and Ions*, VCH Publishers, New York, 1996, pp 245-274.
[16] W. Jeitschko, R.O. Altmeyer, M. Schelk, U.C. Rodewald, *Z. Anorg. Allg. Chem.* 627 (2001) 1932-1940.
[17] I.D. Brown, in: M. O'Keeffe, A. Navrotsky (Eds.), *Structure and Bonding in Crystals*, Vol. 2, Academic Press, New York, 1981, pp 1-30.
[18] M. O'Keeffe, N.E. Brese, *J. Am. Chem. Soc.* 113 (1991) 3226-3229.

Proceeding of the IX International Conference on Crystal Chemistry of Intermetallic Compounds, Lviv, September 20-24, 2005.